RSC Advances

PAPER

View Article Online
View Journal | View Issue

Cite this: *RSC Adv.*, 2015, **5**, 30640

Acid-responsive intracellular doxorubicin release from click chemistry functionalized mesoporous silica nanoparticles

Yue Yan,[a] Jie Fu,*[a] Xin Liu,[a] Tianfu Wang*[b] and Xiuyang Lu[a]

Received 2nd January 2015
Accepted 20th March 2015

DOI: 10.1039/c5ra00059a

www.rsc.org/advances

Anti-tumor drug doxorubicin has been successfully anchored onto MCM-41-type mesoporous silica nanoparticles (MSNs) with acid-cleavable citraconic bond to afford the hybrid Dox–MSN nanomedicine. "click chemistry" has been exploited as an effective method for doxorubicin conjugation. Under normal plasma pH conditions (pH = 7.4), doxorubicin was covalently tethered to the surface of MSNs, avoiding premature drug release when unnecessary. After exposure to acidic microenvironment, such as encountered in cancerous tissue or intracellular compartment endosome, the acid-labile citraconic bond was decomposed, releasing the active pharmaceutical ingredient, doxorubicin. The kinetic profiles of doxorubicin release have been studied under different pH conditions (ranging from 4 to 7.4), clearly indicating a pH-dependent controlled release behavior. MTT assay with human cervical cancer cells (HeLa) and confocal microscopy were used to study the anti-tumor activity and particle uptake behavior of Dox–MSN, respectively. A multitude of physicochemical analytical methods, including TEM, SEM, XRD, porosity analysis, IR spectroscopy, confirmed the successful fabrication of desired MSNs. These acid-responsive MSNs can be speculated to find wide ranging applications as nano-carriers in biomedical research, especially for targeted anticancer drug delivery.

1. Introduction

Due to their intriguing physicochemical properties such as high surface area, large pore volume and ease for further surface functionalization to incorporate new chemical or biological moieties, mesoporous silica nanoparticles (MSNs) have attracted increasing interest for applications in the biomedical areas during the past decade.[1] Another merit of using MSNs as carriers for drug delivery is the development of synthetic strategies to easily fabricate MSNs with controllable size between 30 nm and 200 nm suitable for tumor targeting *via* enhanced permeation and retention effect (EPR).[2,3] Ambrogio *et al.* contributed to this field by first introducing the concept of "capping" strategies to construct "stimuli-responsive" drug delivery systems (DDS) for controlled release of various pharmaceutical agents such as anticancer drugs and DNAs.[4] Thereafter, numerous research groups have reported that MSNs based DDS can release the preloaded cargo at either external or internal stimulus.[5–9]

MSN systems with different release mechanisms have been well investigated,[10] different triggering mechanism for the release of encapsulated cargo have been employed in this process, including pH,[11–13] enzyme,[4,14,15] redox,[16,17] heat,[18] magnetic field[4] and light,[19–21] to fabricate the stimuli-responsive DDS. Amongst all the investigated systems, pH activated release mechanism represents a promising direction because of the natural occurrence of lower pH micro-environments in diseased sites (*e.g.*, tumor, inflammatory tissue) and intracellular subcellular organelles (*e.g.*, endosome), thereby making these pH gradient triggering strategy attractive. In general, two approaches have been exploited to devise and construct these acidity-triggered release systems, either tethering drugs onto the surface of MSNs by acid-labile bonds or encapsulating drugs inside the pores with an acid-activatable "gate-keeper". Using the first approach, Bein *et al.* reported anti-tumor drug can be covalently linked to MSN surface *via* an acetal group and be released upon the acidification of the solution.[22] In another report, Lee *et al.* attached antitumor drug doxorubicin onto MSN walls with acid-sensitive hydrozone linkers and demonstrated their improved liver targeting and subsequent release of the payload.[23] Additionally, acid-responsive MSN-based carriers using nanometer-sized Au,[12] CdS,[24] and β-cyclodextrin[11] as capping agents have also been reported.

Click chemistry for the surface functionalization of materials has increasingly drawn research interest recently. Moreover, it is desirable to exploit click chemistry for conjugating

[a]*Key Laboratory of Biomass Chemical Engineering of Ministry of Education, College of Chemical and Biological Engineering, Zhejiang University, Hangzhou 310027, China. E-mail: jiefu@zju.edu.cn; Fax: +86 571 87952683; Tel: +86 571 87952683*

[b]*Xinjiang Technical Institute of Physics and Chemistry, Chinese Academy of Sciences, Urumqi 830011, China. E-mail: tianfuwang@ms.xjb.ac.cn; Fax: +86 991 3835823; Tel: +86 991 3835823*

therapeutic agents to MSN surfaces due to the mild reaction conditions of alkyne–azide click chemistry and its very high efficiency. As such, click strategy not only allows for mild drug immobilization minimizing the likelihood of drug degradation but also results in high drug loading. Despite click chemistry for covalent immobilization of enzyme has been described elsewhere,[25] strategies that combine the advantages of using click chemistry as a highly efficient, and mild drug loading method and acid-responsive linker as a release mechanism is yet to be reported. To the best of our knowledge, no report has examined MSN based delivery vehicle that can meet these two distinct requirements simultaneously. Thus, it is imperative to design and construct MSNs to withhold payloads covalently linked on the surface when circulating in the reticuloendothelial system (RES) to minimize premature drug release. While the MSNs approach the acidic tumor region or enter endosome or lysosome sub-cellular compartments, the acid-responsive bonds can be decomposed by the pH gradient, facilitating the localized drug delivery.

Herein, we report the development of a novel pH-responsive MSN drug delivery system with improved targeting across multiple length scales in biological microenvironments. We set out to exploit the comparably acidic environment in regions of endosomal and lysosomal intracellular compartments, or tumor growth where the dysfunctional biological cascade systems generated an acidic pH gradient. It is advantageous to harness the lower pH environment in tumor due to the ubiquitous occurrence of the acidic environments in various tumor types.

2. Experimental

Mesoporous silica materials were prepared according to a previously reported method.[8] Tetraethyl orthosilicate and the surfactant *N*-cetyltrimethylammonium bromide (CTAB) were mixed in an aqueous solution containing sodium hydroxide as the catalyst for silica precursor hydrolysis to obtain MSN. The template was removed in a refluxing methanol solution (150 mL) containing 1.5 mL concentrated hydrochloric acid. Aminopropyl functionalized MSN (AP-MSN) was obtained by a post-synthetic grafting method. Subsequently, alkyne-terminated MSN was synthesized by reacting AP-MSN with 4-pentynoic acid. Doxorubicin was first conjugated to citraconic anhydride modified with an azide group, enabling the alkyne–azide click chemistry initiated by freshly prepared Cu(I) in an aqueous media as the catalyst. Similarly, FITC-labeled MSNs were also prepared based on a slightly modified procedure to allow for cellular uptake studies by confocal microscopy.

The following compounds were of analytical grade and were used in this study as received form without further purification: *N*-cetyltrimethylammonium bromide (Sigma), fluorescein isothiocyanate (Sigma), L-ascorbic acid (Sigma), tetraethoxysilane (Aldrich), 3-aminopropyltrimethoxysilane (Aldrich), 4-pentynoic acid (Aldrich), EDC hydrochloride (Fluka), sodium hydroxide (Sinopharm), hydrochloric acid (Sinopharm), methanol (Sinopharm), toluene (Sinopharm), sodium bicarbonate (Sinopharm), copper(II) sulfate pentahydrate (Sinopharm), acetonitrile (Shanghai Lingfeng), sodium azide (Xinxiang), doxorubicin (Hisun pharm).

2.1 Synthesis of MSN

To synthesize MSN materials, 1.00 g *N*-cetyltrimethylammonium bromide (CTAB, 2.74 mmol) was first dissolved in 480 mL of deionized water followed by the addition of 3.50 mL sodium hydroxide aqueous solution (2.00 M). Afterwards, the solution temperature was adjusted to 353 K and stirred at 600 rpm by isotemp digital stirring hot plate. 5.00 mL of the silica precursor, tetraethoxysilane (TEOS, 22.4 mmol), was added dropwise to the solution under vigorous stirring over approximately 15 min. The mixture was kept under 353 K for another 2 h to yield the white precipitate. This solid product was then filtered, washed with copious amount of deionized water and methanol, and dried under high vacuum to yield the as-synthesized surfactant-containing MSN. To remove the surfactant template (CTAB), 1.50 g of the as-synthesized MSN was refluxed (343 K) for 6 h in a 150 mL methanolic solution containing 1.50 mL HCl solution (37.2%). The resulting material was filtered and extensively washed with deionized water and methanol sequentially. The surfactant-free MSN material was placed under high vacuum with heating at 333 K to remove the remaining solvent from the mesopores.

2.2 Synthesis of AP-MSN

As-synthesized 1.00 g MSN was refluxed for 10 h in 80.0 mL anhydrous toluene solution containing 1.00 mL (5.67 mmol) of 3-aminopropyltrimethoxysilane. The synthesized solid 3-aminopropyl-functionalized MSN (AP-MSN) material was then filtered and extensively washed with anhydrous toluene and methanol, followed by high vacuum drying with heating at 353 K overnight.

2.3 Labeling of MSN

FITC labeled MSN materials were synthesized by the co-condensation method. First, 12.0 mg fluorescein isothiocyanate (FITC) was mixed with 0.2 mL 3-aminopropyltrimethoxysilane (APTMS) in 1.0 mL methanol for 2 h at room temperature. 1.00 g *N*-cetyltrimethylammonium bromide (CTAB, 2.74 mmol) and 3.50 mL sodium hydroxide solution (2.00 M) were introduced to 480 mL deionized water and the temperature of the mixture was set to 353 K. Tetraethoxysilane (TEOS, 5.00 mL, 22.4 mmol) was added dropwise to the surfactant-containing solution at a rate of 20 mL h^{-1} under vigorous stirring. Then FITC–APTMS/methanol solution was introduced quickly to the MSN solution. The mixture was allowed to react for 2 h to yield a yellow precipitate. The solid materials were dried under high vacuum. To remove the surfactant template (CTAB), 1.50 g of the as-synthesized FITC–MSN was refluxed (343 K) for 6 h in a 150 mL methanolic solution consisting of 1.50 mL HCl solution (37.2%). The resulting material was filtered and extensively washed with deionized water and methanol sequentially. The surfactant-free FITC–MSN material was placed under high vacuum with

heating at 333 K to remove the remaining solvent from the mesopores.

2.4 Synthesis of Dox–MSN

To synthesize alkyne-terminated MSN, 0.5 g AP-MSN (FITC labeled) and an aqueous solution of 4-pentynoic acid (2.5 mmol) was added into 50 mL $NaHCO_3$ (0.1 M) solution. Subsequently, an amount of 100 mg EDC hydrochloride and NaOH (molar ratio of 1 : 1) was added as a catalyst for the amidation reaction. The solution pH was adjusted above 8, after which the reaction was allowed to proceed at room temperature overnight. The as-prepared material was filtered and extensively washed with deionized water and methanol. Then, it was placed under high vacuum with heating at 353 K overnight.

In order to synthesize the Dox–ligand adduct, 1 mmol Dox (doxorubicin) was dissolved in water and the pH was adjusted to 9.4 by the addition of aqueous NaOH solution. The ligand dissolved in acetonitrile was added dropwise. The resultant solution containing both Dox and ligand was further reacted for 12 h at room temperature. Chromatography was used to purify the Dox–ligand adduct.

The "click chemistry" was employed to conjugate Dox onto the surface of MSN materials. To a solution containing 7 mg of Dox–ligand in PBS buffer (pH 7.4), an amount of 50 mg alkyne-terminated MSN was introduced. 1 mg ascorbic acid was added to 5 mL freshly prepared aqueous $CuSO_4 \cdot 5H_2O$ (1 mM) solution and the resultant solution was stirred at room temperature for 10 min. Subsequently, 12.5 μL of the copper-containing solution was added to initiate the click reaction. The mixed solution was further reacted at 4 °C for 24 h. The Dox–MSN hybrid material was recovered by filtration and washed five times with 20 mL PBS buffer solution (50 mM, pH 7.1).

2.5 Characterization of MSNs

In order to confirm the hexagonal arrangement of the pore structure, small angle X-ray diffraction patterns of the MSN materials were obtained in a powder diffractometer (APEXII, Bruker) using Cu Kα irradiation. Surface area and pore size/volume analysis of the synthesized MSN materials were performed by nitrogen sorption isotherms at 77 K with a Micromeritics Tristar sorptometer. The surface areas were calculated by the Brunauer–Emmett–Teller (BET) method and the pore size distribution were calculated based on the Barrett–Joyner–Halenda (BJH) method. Transmission electron microscopy (TEM) was examined using a JEM-2010 (HR) instrument, operated at 200 kV. For the sample preparation, 1 mg of MSN powder was sonicated in methanol for 10 min. A drop of the suspension was carefully placed on a lacey carbon coated copper TEM grid and dried by a heating lamp for the methanol to evaporate. IR spectroscopy was used to confirm the efficiency of Dox conjugation.

2.6 HPLC profile of MSNs under different pH conditions

Dox–MSN particles was dispersed at buffer solution of different pH values (pH = 4.0, 5.0, and 7.4). At specified times (0, 0.5, 1, 2, 4, 6, 8, and 12 h), an aliquot of solution was withdrawn for released Dox quantification using HPLC (Agilent 1100). A phenomenex Gemini C18 column (4.6 mm inner diameter × 250 mm length) was used. Water–methanol (30 : 70, v/v) with a flow rate at 0.5 mL min^{-1} was used as mobile phase. The temperatures of the column were kept at 30 °C, and the wavelength of UV detector was chosen at 480 nm.

2.7 Toxicity measurement of Dox–MSN using HeLa cells

HeLa cells were maintained in RPMI 1640 (GIBCO) supplemented with 10% heat-inactivated fetal bovine serum (GIBCO), penicillin (100 units per mL) and streptomycin (100 μg mL^{-1}) in a humidified atmosphere of 5% CO_2 at 37 °C. The cytotoxicity of Dox–MSN was determined by 3-(4,5-dimethylthiazol-2-yl)-2,5-diphenyltetrazolium bromide (MTT) assay. Cells were seeded in 96-well plates at a density of 4000 cells per well in 200 μL of 10% FBS containing cell culture medium and incubated overnight. Dox–MSN were added at concentration of 0, 1, 10, 25, 50, and 100 μg mL^{-1} and further incubated for 48 h. The medium in each well was replaced with fresh culture medium containing 0.75 mg mL^{-1} MTT. After an additional incubation of 3 h, allowing viable cells to reduce the yellow tetrazolium salt (MTT) into dark blue formazan crystals, the medium was replaced by 100 μL DMSO to dissolve the formazan crystals. The absorbance was detected at 562 nm using the microplate spectrophotometer (SpectraMax M2E, Molecular Device Inc. USA).

2.8 Time-lapse live cell imaging

Time-lapse microscopy was performed using a Delta Vision microscope system (Applied Precision, Issaquah, WA, USA). 231 cells were seeded at the density of 1×10^5 cells per well in 24 well plates in 0.5 mL 1640 medium with coverslips at the bottom of the wells and cultured for 24 h at 37 °C with 5% CO_2. After 24 h of incubation, the 1640 medium was replaced by 0.5 mL of MSNs (40 μg mL^{-1}) in the serum-free 1640 medium for 12 h. The cell-plated coverslips were then washed with PBS buffer (pH 7.4). The coverslips at the bottom of the wells were added to 4% paraformaldehyde and cultured for 15 min at 37 °C, followed by carefully rinsing with PBS for three times. Finally, 0.5% Triton 100 was added to culture for 15 min at 37 °C, followed by carefully rinsing with PBS for three times. Before cell imaging, cells were stained with 5.7 μM 4′,6-diamidino-2-phenylindole (DAPI) and cultured for 15 min at 37 °C, followed by carefully rinsing with PBS for three times. Immediately thereafter, fluorescence quenching agent was added to the coverslips. The DAPI-stained coverslips were measured using a 40× objective, with wavelengths from 340 to 458 nm. Likewise, green fluorescent FITC–MSN particles, red fluorescent Dox, and Dox–MSN conjugates were also measured. Obtained imaging data was processed using Delta Vision SoftWoRx software.

3. Results and discussion

As shown in Fig. 1, through EPR effects, MSNs bearing doxorubicin can selectively be enriched in tumor region where the newly formed vascular are inherently porous and allows for

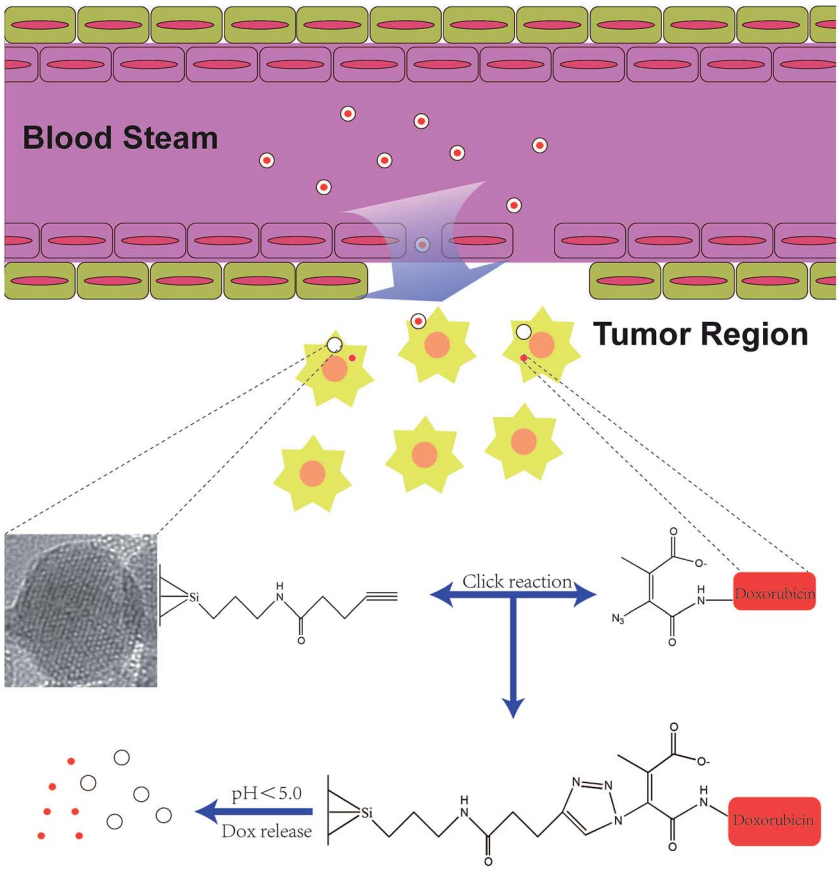

Fig. 1 Illustration of acid-responsive doxorubicin release from MSN.

MSN accumulation. Subsequently, MSNs enter cancer cell *via* endocytosis mechanism, enabling the contact of the acid-responsive citraconic bonds and protons found in both endosomes and lysosomes. Upon cleavage of the acid-labile bonds, doxorubicin bound on the inside channels and outmost surface of MSNs can be released to take effect.

The results of nitrogen sorption analysis showed that surface area and pore volume of MSN material both decreased after doxorubicin loading. For instance, BET surface area decreased from 1037.96 $m^2\ g^{-1}$ to 45.79 $m^2\ g^{-1}$, while pore volume also reduced from 0.99 $cm^3\ g^{-1}$ to 0.196 $cm^3\ g^{-1}$. These results demonstrated the successful functionalization of MSN with doxorubicin molecules.

As seen in Fig. 2, transmission microscopy (TEM) revealed the synthesized MSNs have a spherical morphology with an average diameter of 100–200 nm. MSNs within this size range are suitable for EPR mediated targeting due to newly formed blood vessel in most solid tumor types have vascular pore size cut-off starting at about 400 nm. X-ray diffraction (XRD) analysis showed a main peak attributed to [100] reflection from hexagonally packed mesopores (Fig. 3). In addition, higher order reflections of [110] and [200] were also present for these MCM-41-type materials.

IR spectroscopy was performed to study the organic functionalities on the surface of various MSN materials. As shown in Fig. 4, the N–H bending mode at about 1560 cm^{-1} and the

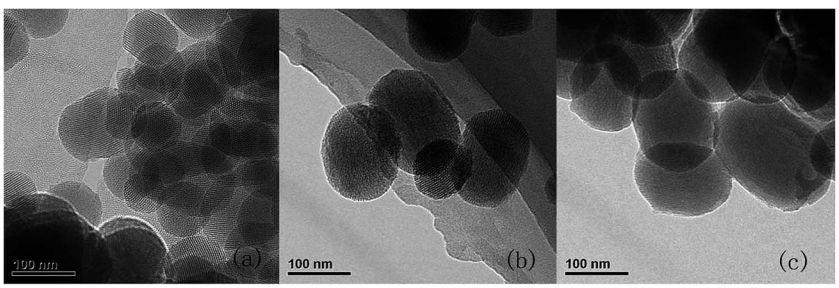

Fig. 2 Transmission electron micrograph (TEM) of (a) MSN; (b) AP-MSN; (c) Dox–MSN.

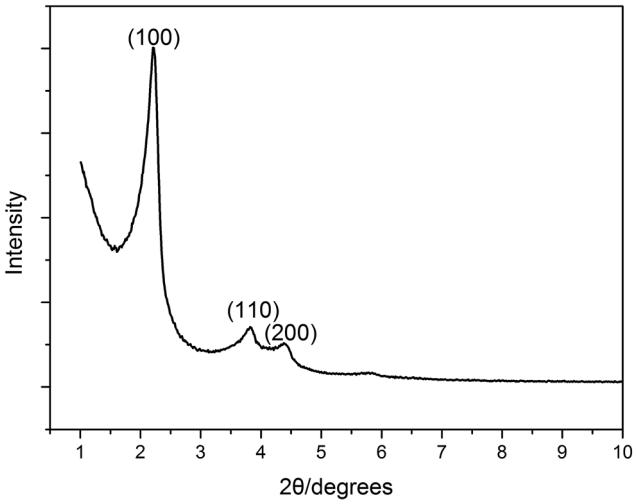

Fig. 3 Low angle X-ray diffraction pattern of MSN.

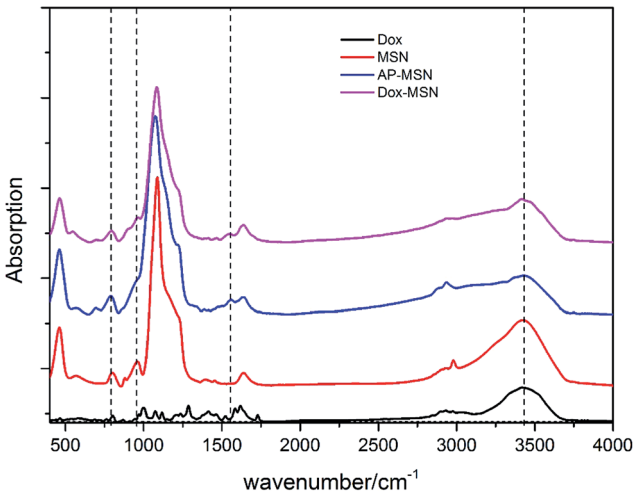

Fig. 4 IR spectra of the samples of MSN (red line), AP-MSN (blue line), Dox–MSN (purple line), Dox (black line).

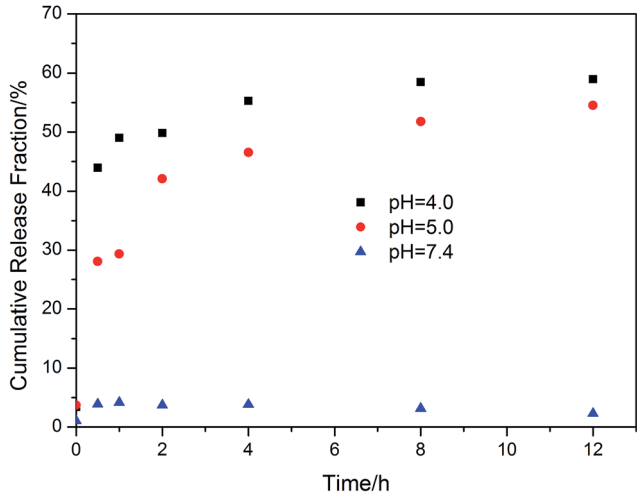

Fig. 5 Release profiles of Dox from MSN at pH 4.0 (black squares), pH 5.0 (red dots), pH 7.4 (blue triangles).

almost disappearance of hydroxyl stretch (960 cm^{-1}) are attributed to the amino groups of 3-aminopropyl group. After click chemistry functionalization, the disappearance of the amino stretch on intact MSN and the N–H bending mode strength of the MSN and the Dox–MSN at about 800 cm^{-1} are almost the same and apparently lower than that of AP-MSN, indicating the successful functionalization of MSN with doxorubicin molecule.

Several different pH values (pH = 4, 5 and 7.4) were chosen to mimic the acidic environment and normal plasma condition to study the release kinetic profiles of these Dox–MSN *in vitro*. The Dox–MSN particles were immersed in different pH buffers with stirring and an aliquot of aqueous samples were taken at specified times over a period of 12 h. As shown in Fig. 5, under pH of 7.4, doxorubicin was barely released throughout the studied time period. However, under acidic environments such as those of pH at 4 and 5, most of attached doxorubicin were gradually released, indicating the effectiveness of the designed acid-responsive release mechanism. Cell viability in contact with different concentrations of Dox–MSNs was investigated to explore the biological effectiveness of the nanoparticles bearing the drugs. As shown in Fig. 6, after 48 h of incubation, the percentage of live cells decreased as Dox–MSN particle concentration increased. At a Dox–MSN dosage of 100 μg mL^{-1}, about 50% cells were alive, meanwhile about 37.9% cells were alive at the same concentration of equivalent Dox. These results showed that MSN–Dox conjugates retained similar biological effectiveness of free Dox while minimizing premature release of Dox at undesired locations within the body. Whereas previous studies showed that bare MSN particles at 100 μg mL^{-1} concentration had very little effect on cell growth.[26] This comparison suggested that the drug–nanoparticle conjugates were effective agents inhibiting tumor cell growth *in vitro*.

Time-lapse microscopy was performed to probe the endocytosis behavior of Dox–MSN nanoparticles and the results were

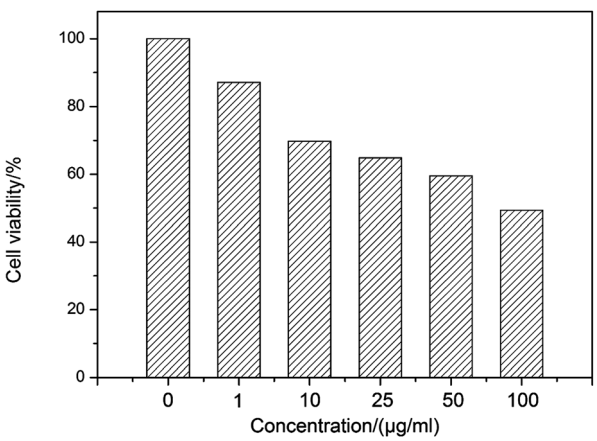

Fig. 6 Cellular viability studies with Dox–MSN. Different concentrations of Dox–MSNs (ranging from 0 to 100 μg mL^{-1}) in culture media were used.

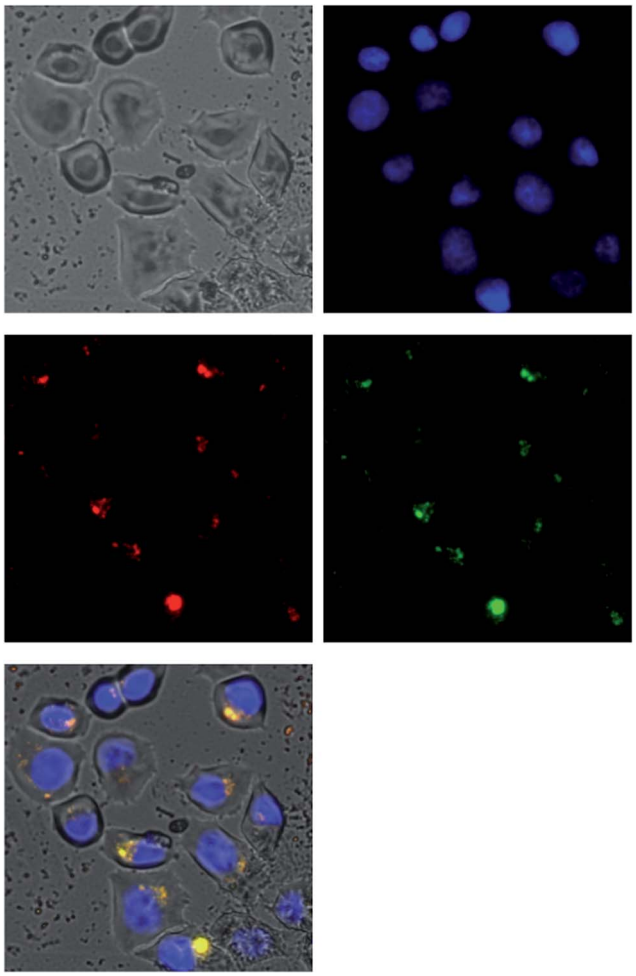

Fig. 7 Time-lapse live cell imaging of Dox–MSN nanoparticle suspension (40 μg mL^{-1}) (a) cultured cell; (b) DAPI-stained nuclei; (c) Dox; (d) FITC-stained Dox–MSN; (e) overlapping of (b–d).

summarized in Fig. 7. Fig. 7b–d demonstrated the DAPI-stained nuclei in blue, doxorubicin in red, and FITC-labeled Dox–MSN in green, respectively. In addition, Fig. 7e is the overlapping of Fig. 7b–d, from which it can be observed that some Dox–MSN nanoparticles were in close proximity to the nuclei where biological effects of doxorubicin is preferred to occur. These results were in agreement with previous report where MSNs were demonstrated to be capable of escaping endosome to release the attached pharmaceutical agents to the cytoplasm.[1] Moreover, as seen in Fig. 7e, some red spots were found throughout the cell, indicating the presence of detached doxorubicin. This information suggested that the acid-responsiveness design not only worked in simulated endosomal pH conditions but also was effective in the cell culture experiments.

4. Conclusion

PH-responsive MSNs bearing antitumor drug, doxorubicin, were successfully constructed. Upon exposure to simulated acidic environment, doxorubicin can be readily detached and released from Dox–MSN nanoparticles within a couple of hours whereas under normal plasma pH condition of 7.4, the drug was barely released. To further probe the Dox–MSN drug delivery system, cell viability analysis using a MTT method was conducted, demonstrating the effectiveness of Dox–MSN to inhibit cell growth by 50% at a concentration of 100 μg mL^{-1}, at which bare MSN particles were previously found to be compatible with cell growth. In addition, live cell imaging was conducted to study the endocytosis and localization behavior of Dox–MSNs and it was observed that the nanoparticles can successfully escape endosome and finally reach the nuclei for the drug to perform biological effects. Although a couple of other factors such as biocompatibility and circulating time need to be considered to further apply the Dox–MSN nanoparticles for practical drug delivery application, the successful fabrication in the current study demonstrated a facile method to synthesize acid-responsive drug–MSN conjugates, which can be speculated to have potential in a wide range of biomedical applications.

Acknowledgements

This work was supported by the National Natural Science Foundation of China (no. 21306165, 21176218, U1139302), Zhejiang Provincial Natural Science Foundation of China (no. LZ14B060002, LQ13B060001) and Chinese government 1000 plan program (Y42H291501).

References

1 I. I. Slowing, B. G. Trewyn, S. Giri and V. S. Y. Lin, *Adv. Funct. Mater.*, 2007, **17**, 1225–1236.
2 I. I. Slowing, J. L. Vivero-Escoto, C.-W. Wu and V. S. Y. Lin, *Adv. Drug Delivery Rev.*, 2008, **60**, 1278–1288.
3 B. G. Trewyn, I. I. Slowing, S. Giri, H.-T. Chen and V. S. Y. Lin, *Acc. Chem. Res.*, 2007, **40**, 846–853.
4 M. W. Ambrogio, C. R. Thomas, Y.-L. Zhao, J. I. Zink and J. F. Stoddart, *Acc. Chem. Res.*, 2011, **44**, 903–913.
5 J. L. Vivero-Escoto, R. C. Huxford-Phillips and W. Lin, *Chem. Soc. Rev.*, 2012, **41**, 2673–2685.
6 S. Huh, J. W. Wiench, B. G. Trewyn, S. Song, M. Pruski and V. S. Y. Lin, *Chem. Commun.*, 2003, 2364–2365, DOI: 10.1039/b306255d.
7 B. G. Trewyn, C. M. Whitman and V. S. Y. Lin, *Nano Lett.*, 2004, **4**, 2139–2143.
8 C.-Y. Lai, B. G. Trewyn, D. M. Jeftinija, K. Jeftinija, S. Xu, S. Jeftinija and V. S. Y. Lin, *J. Am. Chem. Soc.*, 2003, **125**, 4451–4459.
9 J. Lu, E. Choi, F. Tamanoi and J. I. Zink, *Small*, 2008, **4**, 421–426.
10 Z. Li, J. C. Barnes, A. Bosoy, J. F. Stoddart and J. I. Zink, *Chem. Soc. Rev.*, 2012, **41**, 2590–2605.
11 H. Meng, M. Xue, T. Xia, Y.-L. Zhao, F. Tamanoi, J. F. Stoddart, J. I. Zink and A. E. Nel, *J. Am. Chem. Soc.*, 2010, **132**, 12690–12697.
12 R. Liu, Y. Zhang, X. Zhao, A. Agarwal, L. J. Mueller and P. Feng, *J. Am. Chem. Soc.*, 2010, **132**, 1500–1501.

13 Q. Gan, X. Lu, Y. Yuan, J. Qian, H. Zhou, X. Lu, J. Shi and C. Liu, *Biomaterials*, 2011, **32**, 1932–1942.
14 A. Schlossbauer, J. Kecht and T. Bein, *Angew. Chem., Int. Ed.*, 2009, **48**, 3092–3095.
15 K. Patel, S. Angelos, W. R. Dichtel, A. Coskun, Y.-W. Yang, J. I. Zink and J. F. Stoddart, *J. Am. Chem. Soc.*, 2008, **130**, 2382–2383.
16 R. Mortera, J. Vivero-Escoto, I. I. Slowing, E. Garrone, B. Onida and V. S. Y. Lin, *Chem. Commun.*, 2009, 3219–3221, DOI: 10.1039/b900559e.
17 B. Chang, D. Chen, Y. Wang, Y. Chen, Y. Jiao, X. Sha and W. Yang, *Chem. Mater.*, 2013, **25**, 574–585.
18 Z. Zhou, S. Zhu and D. Zhang, *J. Mater. Chem.*, 2007, **17**, 2428–2433.
19 S. Angelos, Y.-W. Yang, N. M. Khashab, J. F. Stoddart and J. I. Zink, *J. Am. Chem. Soc.*, 2009, **131**, 11344–11346.
20 J. Lai, X. Mu, Y. Xu, X. Wu, C. Wu, C. Li, J. Chen and Y. Zhao, *Chem. Commun.*, 2010, **46**, 7370–7372.
21 N. Z. Knezevic, B. G. Trewyn and V. S. Y. Lin, *Chem. Commun.*, 2011, **47**, 2817–2819.
22 A. Schlossbauer, C. Dohmen, D. Schaffert, E. Wagner and T. Bein, *Angew. Chem., Int. Ed.*, 2011, **50**, 6828–6830.
23 C.-H. Lee, S.-H. Cheng, I. P. Huang, J. S. Souris, C.-S. Yang, C.-Y. Mou and L.-W. Lo, *Angew. Chem., Int. Ed.*, 2010, **49**, 8214–8219.
24 N. Z. Knezevic and V. S. Y. Lin, *Nanoscale*, 2013, **5**, 1544–1551.
25 A. Schlossbauer, D. Schaffert, J. Kecht, E. Wagner and T. Bein, *J. Am. Chem. Soc.*, 2008, **130**, 12558–12559.
26 J. Vivero-Escoto, I. Slowing, B. Trewyn and V. Lin, *Small*, 2010, **6**, 1952–1967.